

UB CCD PHOTOMETRY OF THE OLD, METAL RICH, OPEN CLUSTERS NGC 6791, NGC 6819 AND NGC 7142

G. CARRARO¹

European Southern Observatory, Alonso de Cordova 3107, Casilla 19001, Santiago 19, (Chile)

A. BUZZONI

INAF - Osservatorio Astronomico di Bologna, Via Ranzani 1, 40127 Bologna (Italy)

E. BERTONE

INAOE - Instituto Nacional de Astrofísica Óptica y Electrónica, Calle L.E. Erro 1, 72840 Tonantzintla, Puebla (Mexico)

AND

L. BUSON

INAF - Osservatorio Astronomico di Padova, Vicolo Osservatorio 5, 35122 Padova (Italy)

ABSTRACT

We report on a UV-oriented imaging survey in the fields of the old, metal-rich open clusters, NGC 6791, NGC 6819 and NGC 7142. With their super-solar metallicity and ages $\gtrsim 3$ -8 Gyr, these three clusters represent both very near and ideal stellar aggregates to match the distinctive properties of the evolved stellar populations, as in elliptical galaxies and bulges of spirals. Following a first discussion of NGC 6791 observations in an accompanying paper, here, we complete our analysis, also presenting for NGC 6819 and NGC 7142 the first-ever U CCD photometry. The color magnitude diagram of the three clusters is analyzed in detail, with special emphasis to the hot stellar component. We report, in this regard, one new extreme horizontal-branch star candidate in NGC 6791. For NGC 6819 and 7142, the stellar luminosity function clearly points to a looser radial distribution of faint lower Main Sequence stars, either as a consequence of cluster dynamical interaction with the Galaxy or as an effect of an increasing fraction of binary stars toward the cluster core, as actually observed in NGC 6791 too. Compared to a reference theoretical model for the Galaxy disk, the analysis of the stellar field along the line of sight of each cluster indicates that a more centrally concentrated thick disk, on a scale length shorter than ~ 2.8 kpc, might better reconcile the lower observed fraction of bright field stars and their white-dwarf progeny.

Subject headings: open clusters and associations: general - open clusters and associations: individual (NGC 6791, NGC 6891, NGC 7142) - stars: evolution

1. INTRODUCTION

Old open clusters are widely recognized as valuable tools to study the stellar population of the Galactic thin disk (Bragaglia & Tosi 2006; Carraro et al. 2007) and, at the same time, as important benchmarks to probe stellar structure and evolution theories. Recently, much attention has been paid to the evolution of stars along the red giant branch (RGB), and the role of metallicity as main driver of mass loss (e.g. van Loon 2006; Origlia et al. 2007) and possible origin of extended blue horizontal branch (BHB) stars. In this context old, metal rich, open clusters are ideal targets and, among these, NGC 6791 certainly stands out for its conspicuous population of blue horizontal-branch (BHB) stars (Kaluzny & Rucinski 1995; Brown et al. 2006), and a wealth of white dwarfs (WD) (Bedin et al. 2008). However, the lack of high-quality UV photometry, particularly in the U band, prevented so far a full characterization of the BHB component both in terms of completeness and UV

properties.

This is the main scope of the present study, in which we present accurate wide-field UB photometry across the cluster NGC 6791. This photometric material provided the reference for Buzzoni et al. (2012) to characterize the UV properties of this cluster leading to conclude that it can robustly be considered as a nearby proxy of the elliptical galaxies displaying a strong UV-upturn phenomenon. However, a detailed description of the photometric data, their reduction and calibration, was deferred to the present paper. Together with NGC 6791, we are going to present here UB photometry for two additional old, likely metal-rich, open clusters, namely NGC 6819 and NGC 7142, for which CCD U photometry is not available so far. The main aim is to describe the color-magnitude diagram (CMD) in these pass-bands and, in case, assess the possible presence of BHB candidate stars.

1.1. NGC 6791

Besides NGC 188, this object is the only relatively close system known to contain a sizable fraction of sdB stars (Landsman et al. 1998). Located less than 5 kpc away (Carraro et al. 1999, 2006; Carney et al. 2005), it stands out as a treasured “Rosetta Stone” to assess the UV emission of more distant ellipticals (Buzzoni et

Electronic address: gcarraro@eso.org
 Electronic address: alberto.buzzoni@oabo.inaf.it
 Electronic address: ebertone@inaoep.mx
 Electronic address: lucio.buson@oapd.inaf.it

¹ On leave from Dipartimento di Fisica e Astronomia, Università di Padova, Italy

al. 2012). Though the first detailed study of NGC 6791 goes back to the work of Kinman (1965), its truly peculiar hot-HB content has indeed been recognized a few decades later, when Kaluzny & Udalski (1992) (hereafter, KU92) as well as Kaluzny & Rucinski (1995) (hereafter, KR95) verified that it hosts a significant fraction of sdB/O stars. Later, Yong & Demarque (2000) interpreted these hot sources as extreme horizontal-branch (EHB) stars with T_{eff} in the range 24–32 000 K, as also confirmed by ground and space-borne (UIT and HST) observations (Liebert et al. 1994; Landsman et al. 1998).

Its old age, about 8 Gyr, has recently been confirmed by Anthony-Twarog et al. (2007) using *vbyCaH β* CCD photometry, while a recent estimate of metallicity (i.e. $[Fe/H] \sim +0.40$) has been provided by Carraro et al. (2006), Origlia et al. (2006), and Gratton et al. (2006), relying on high-resolution spectroscopy.

1.2. NGC 6819

A first hint of a relatively old age for this cluster dates almost 30 years ago, from the photographic studies of Lindoff (1972) and Auner (1974), which compared the turnoff and red giant branch location relative to the CMD of the evolved system M 67. More recent and accurate age estimates from deep *BVI* CCD photometry (Carraro & Chiosi 1994; Kalirai et al. 2001; Rosvick & Vandenberg 1998; Warren & Cole 2009) better agree around a value of ~ 3 Gyr. No *U* photometry has been published so far for this cluster.

Chemical abundances from high-resolution spectroscopy of red-clump stars in the cluster have recently been presented by Bragaglia et al. (2001) and Warren & Cole (2009), suggesting a value of $[Fe/H] = +0.09$. This consistently agrees with the original estimate by Twarog et al. (1997), based on Strömgen photometry.

1.3. NGC 7142

The similarity of the NGC 7142 CMD with that of the old open clusters NGC 188 and M 67 has been pointed out by van den Bergh (1962). Specific *BV* CCD photometry has been carried out by Crinklaw & Talbert (1991) pointing to an age of 4–5 Gyr for this cluster, actually intermediate between that of M67 and NGC 188. This estimate matches both the very early observations of van den Bergh (1962) and the more recent results of Carraro & Chiosi (1994). As far as metallicity is concerned, Jacobson et al. (2007, 2008) ascribe to NGC 7142 a moderately super-solar metal content, with $[Fe/H] = +0.14$. The only modern CCD study of this cluster is from Janes & Hoq (2011), in the *BVI* pass-bands, and supports previous estimates for age, distance and reddening.

2. OBSERVATIONS AND DATA REDUCTION

A first CCD *U, B* observing run was carried out with the U-high-sensitive DOLORES optical camera mounted on the 3.6 m Telescopio Nazionale Galileo (TNG) at the Roque de Los Muchachos Observatory of La Palma (Spain). Observations have been carried out along the three nights of July 29–31, 2003. DOLORES was equipped with a 2048×2048 pixels LORAL CCD with a $0''.275$ pixel size. This provided a $9'.4 \times 9'.4$ field of view on the sky. Four slightly overlapping fields were eventually observed across each cluster, covering a total area of

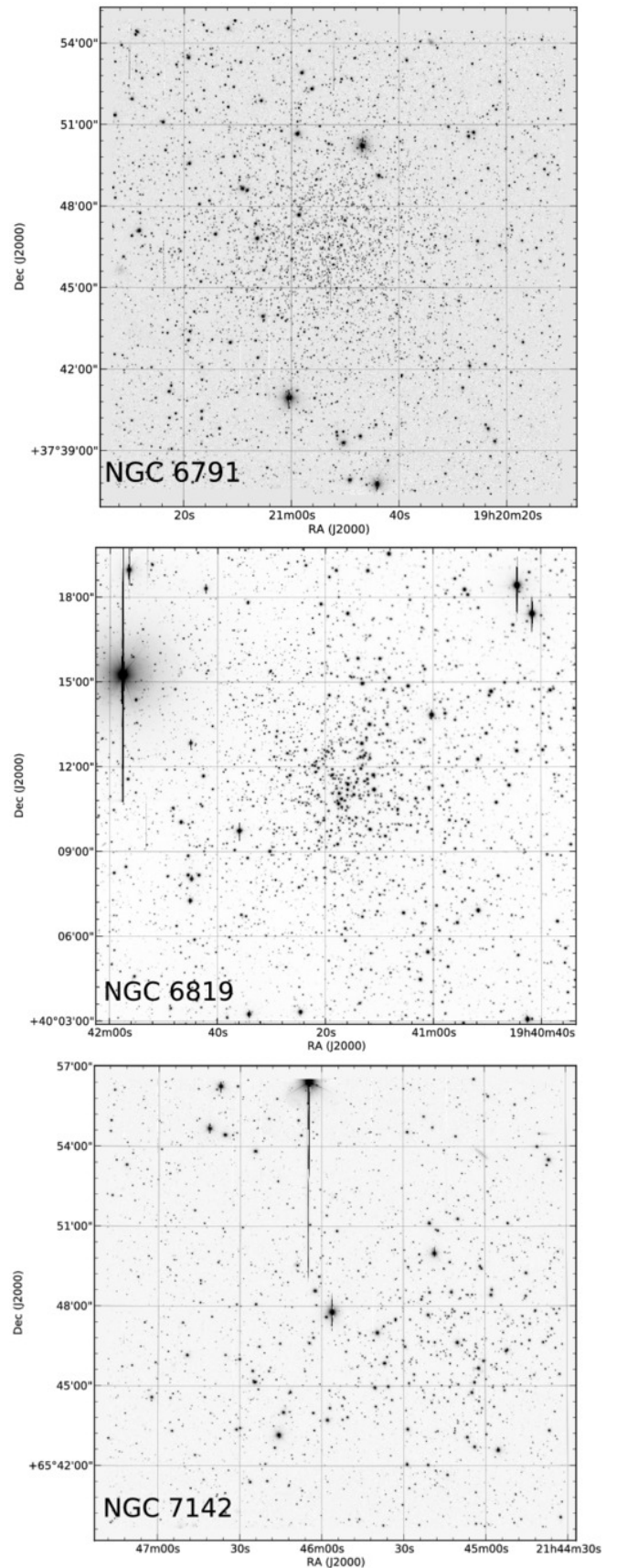


FIG. 1. — B 300 secs mosaics of the 4 pointings for each cluster, NGC 6791, NGC 6819, and NGC 7142, as labelled in each panel. The field of view is 17 arcmin on a side. North is up, East to the left.

TABLE 1
JOURNAL OF OBSERVATIONS FOR THE 2003 RUN

Target	Date	Filter	Exposure sec	airmass	seeing arcsec
NGC 6791	2003 July 29	<i>U</i>	1200	1.02–1.09	0.8
		<i>B</i>	300	1.01–1.13	0.7
PG2213+006		<i>U</i>	2×30	1.14–1.62	0.9
		<i>B</i>	2×10	1.14–1.63	0.8
NGC 6819	2003 July 30	<i>U</i>	1200	1.02–1.16	0.9
		<i>B</i>	300	1.02–1.18	0.8
PG2213+006		<i>U</i>	2×30	1.14–1.62	0.7
		<i>B</i>	2×10	1.14–1.63	0.7
NGC 7142	2003 July 31	<i>U</i>	1200	1.25–1.28	1.0
		<i>B</i>	300	1.25–1.31	1.0
PG2213+006		<i>U</i>	30	1.14–1.62	0.9
		<i>B</i>	10	1.14–1.63	0.8
PG1525+071		<i>U</i>	30	1.14–1.62	0.9
		<i>B</i>	10	1.14–1.63	0.9

roughly $17'.0 \times 17'.0$ (see Fig. 1). The details of the observations are listed in Table 1. A further set of shallower images with 5 seconds exposure time and similar pointing sequence and instrumental setup has subsequently been required to recover saturation effects in the photometry of the brightest stars ($B \lesssim 14$) in the fields. These supplementary data have been kindly provided us for clusters NGC 6819 and 7142 by the TNG service staff along the Oct 2009 observations. Unfortunately, no useful data have been made available for NGC 6791, so that a different correcting procedure had to be devised for this cluster, as we discuss in Sec. 3.1.

Data have been reduced with the IRAF² packages CCDRED, DAOPHOT, ALLSTAR and PHOTCAL using the point-spread-function (PSF) method (Stetson 1987). The three nights along the 2003 run turned out to be photometric and very stable, such as to allow us to derive calibration equations for all of the 20 observed standard stars of the two Landolt (1992) fields.

The calibration equations turned out of be in the form:

$$\begin{aligned} u &= U + u_1 + u_2 * X + u_3 (U - B) \\ b &= B + b_1 + b_2 * X + b_3 (U - B), \end{aligned} \quad (1)$$

where U, B are standard magnitudes, u, b are the instrumental ones and X is the airmass; all the coefficient values are reported in Table 2. Second order terms have also been calculated, but turned out to be negligible (0.005 – 0.015), and therefore not included.

In the case of NGC 6791 the specific goal of this run was to assess the possible presence of additional hot EHB stars *fainter* than $B \sim 17$, that is the magnitude of the seven, UV-enhanced candidates originally reported by KU92. Quite unexpectedly, the preliminary results of these data led Buson et al. (2006) to suspect the presence of a *bright* EHB clump of stars surmounting the KU92 objects. However, a closer scrutiny of the reduced data revealed that most of the newly detected candidates displayed in fact a too high photometric error for their apparent luminosity and they were too close to the B saturation limit of our deep photometry to provide conclusive arguments on their nature as hot sdB stars.

² IRAF is distributed by NOAO, which are operated by AURA under cooperative agreement with the NSF.

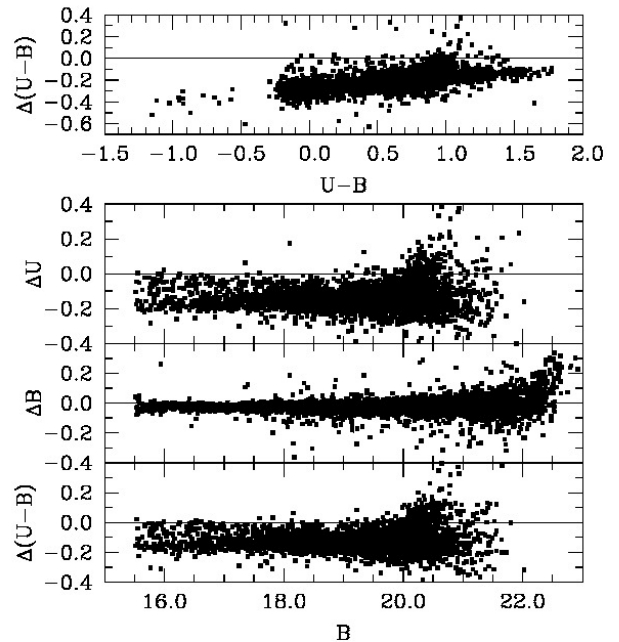


FIG. 2.— U, B cross-correlation of our photometry with KR95 data for cluster NGC 6791. Color and magnitude differences for the 5510 stars in common are displayed in the different panels versus our photometry. Mean zero-point offsets are in the sense (“our photometry” – KR95). Note, in the upper panel, the evident ($U - B$) color drift of KR95 photometry with respect to our data.

TABLE 2
COEFFICIENTS FOR STANDARD MAGNITUDE CALIBRATION

U band	u_1	u_2	u_3
Jul 29	0.341 ± 0.022	0.49 ± 0.02	0.103 ± 0.033
Jul 30	0.349 ± 0.018	0.49 ± 0.02	0.099 ± 0.023
Jul 31	0.367 ± 0.014	0.49 ± 0.02	0.139 ± 0.018
B band	b_1	b_2	b_3
Jul 29	-1.544 ± 0.010	0.25 ± 0.02	0.022 ± 0.014
Jul 30	-1.581 ± 0.013	0.25 ± 0.02	-0.016 ± 0.017
Jul 31	-1.581 ± 0.012	0.25 ± 0.02	-0.004 ± 0.016

2.1. Cross-check with other photometry sources in the literature

Cluster NGC 6791 is the only one with independent UB photometry carried out by KR95, and this provided a valuable opportunity to check our results by cross-correlating the two photometric catalogs. The comparison restrained only to stars fainter than $B = 15.55$ mag, to safely avoid any saturation effect in our magnitude scale. The magnitude and color residuals for the 5510 stars in common with the KR95 dataset are shown in Fig. 2. In these plots the displayed difference is in the sense (“our photometry” – KR95). As evident from the figure, a fairly good agreement is found for the B photometry, with a mean magnitude residual $\langle \Delta B \rangle = 0.064 \pm 0.041$ over the whole star sample. Major discrepancies appear, on the contrary, for the U magnitudes with a larger zero-point offset, namely $\langle \Delta U \rangle = -0.204 \pm 0.177$, and a clear evidence of a color drift (see the upper panel of Fig. 2). One has to remind, in this regard, that KR95 themselves warn about possible systematics with their U filter and apply an *a posteriori* offset to their ($U - B$) color.

An independent settlement of this apparent mismatch

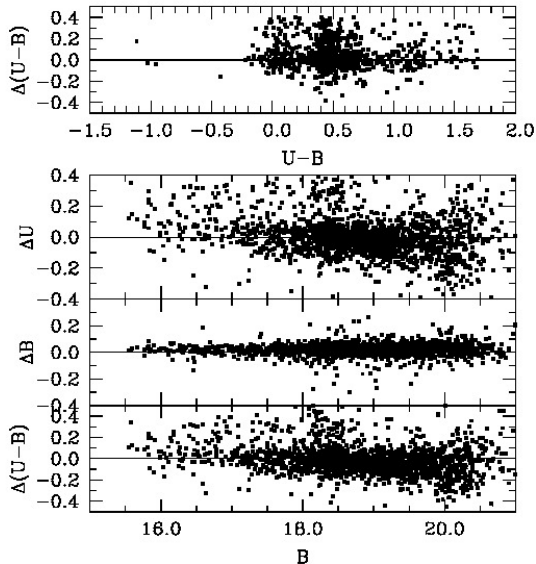


FIG. 3.— Same as Fig. 2, but comparing with Montgomery et al. (1994) CCD magnitudes of 2370 NGC 6791 stars in common with our dataset. Magnitude residuals are in the sense (“our photometry” – Montgomery et al.), and are plotted against our photometry. The vanishing residual distribution in the different panels confirms that our photometry is in the same reference as that of Montgomery et al.

can be attempted by further cross-correlating our photometry with the CCD magnitudes of Montgomery et al. (1994), as shown in Fig. 3. Quite comfortably, the much smaller photometric offsets, i.e. $\langle \Delta B \rangle = 0.021 \pm 0.059$ and $\langle \Delta U \rangle = 0.058 \pm 0.232$, and the lack of any evident color drift for the 2370 stars in common confirm the excellent agreement, thus adding further strength to our photometry with respect to the KR95 results.

2.2. Completeness analysis

By looking at Table 1, one immediately realizes that the three clusters have been observed under the same seeing conditions. However, Fig. 1 shows that NGC 6791 is by far the most crowded cluster, and therefore its photometry is the most affected by crowding/incompleteness effects. Both NGC 6819 and NGC 7142 look less affected by this problem. We therefore investigated incompleteness effects only on NGC 6791 images. Completeness corrections were determined in the standard way by running artificial star experiments on the data, frame by frame, in both U and B filters. Basically, several simulated images were created by adding artificial stars to the original frames. The artificial stars were added at random positions and had the same color and luminosity distribution as the sample of true stars. To cope with potential over-crowding, up to 20% of the original number of stars were added in each simulation. Depending on the frame, between 1500 and 2000 stars were added in this way. The ratio of recovered to inserted stars is a measure of the photometry completeness. The results are summarized in Table 3, and show that both in U and in B the photometry has a completeness value larger than 50% up to 23 mag.

3. CLUSTER CMDS

The DAOPHOT search across the field of our three clusters allowed us to confidently detect and measure magnitude and color for some 18,000 objects brighter than

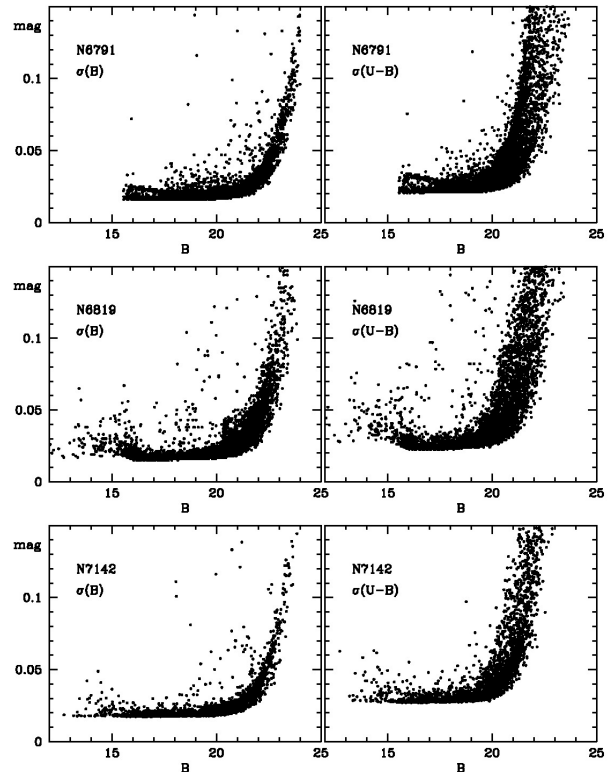


FIG. 4.— B -band internal errors from DAOPHOT photometry in the field of NGC 6791, NGC 6819 and NGC 7142. Where available, “shallow” imagery has been used for the photometry of the brightest ($B \lesssim 15.5$) stars in the fields of NGC 6819 and 7142, as explained in Sec. 2. The bright-end star distribution in the NGC 6791 field, on the contrary, has been recovered from KR95 photometry, as discussed in Sec. 3.1. One can notice that the $B \sim 22$ mag level has been safely reached in the three clusters, mostly within a 0.05 mag accuracy.

TABLE 3
COMPLETENESS STUDY FOR NGC 6791 AS A FUNCTION OF THE FILTER.

Δ Mag	U	B
13-14	100%	100%
14-15	100%	100%
15-16	100%	100%
16-17	100%	100%
17-18	100%	100%
18-19	100%	100%
19-20	100%	100%
20-21	93%	95%
21-22	84%	85%
22-23	70%	73%
23-24	38%	41%

$B \simeq 24.0$ in the fields of the three clusters. Within these magnitude limits, the NGC 6791 sample consisted therefore of 7774 stars, while 7683 and 3422 stars have been picked up in the NGC 6819 and NGC 7142 fields, respectively. A quick-look analysis of the internal photometric uncertainty of our survey can be carried out by means of Fig. 4. From the plots one can appreciate that $B \sim 22$ mag has been safely reached throughout, mostly within a 0.05 mag accuracy. The B versus $(U - B)$ CMDs for our clusters are presented in the series of Figs. 5, 9 and 12.

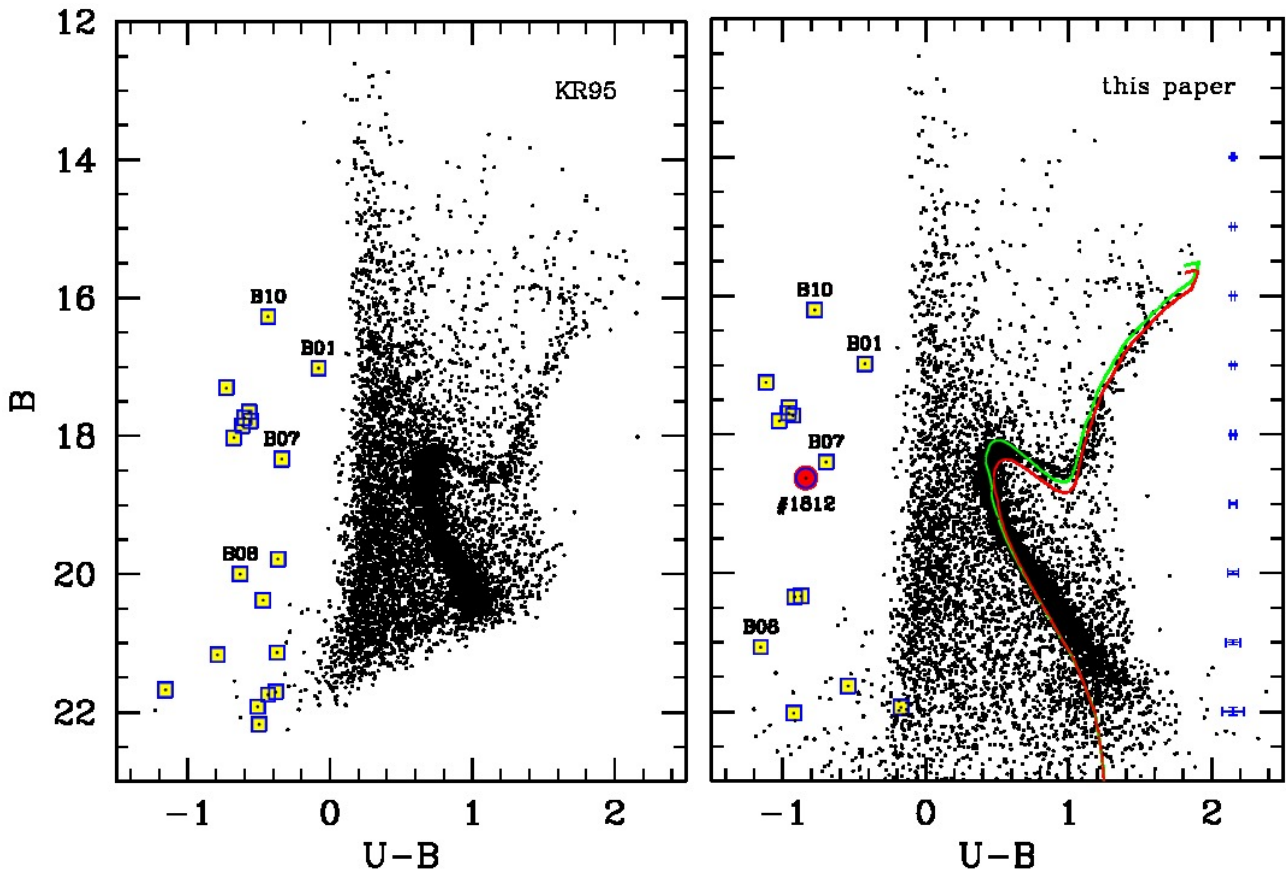


FIG. 5.— Comparison of the B versus $(U - B)$ CMD of NGC 6791 according to Kaluzny & Rucinski (1995) (*left panel*) and the present paper (*right panel*). The KR95 hot-star candidates of Table 4 and 5 (including in particular the outstanding EHB stellar clump about $B \sim 18$) are marked in both plots as big squares. The three controversial cases of stars B01, B07 and B10 are also labelled in the plots, together with stars B08, the hottest object in our sample. The big dot in the right panel indicates the new EHB candidate (ID 1812 in Table 4) we discovered in this study. An illustrative match with the Padova isochrone set (Bertelli et al. 2008) is displayed in the right panel assuming for the cluster an age range between 6 and 8 Gyr and chemical mix $(Z, Y) = (0.04, 0.30)$. The theoretical models have been shifted to an apparent B distance modulus $(m - M)_B = 13.6$ mag and reddened by $E(U - B) = 0.13$. Typical error bars for our photometry at the different magnitude levels are displayed on the right.

3.1. NGC 6791

Our output for the NGC 6791 field is shown in Fig. 5, where we also compare with the Kaluzny & Rucinski (1995) original photometry (Table 2 therein). As we were previously commenting on, the two datasets exhibit zero-points differences in U , which make the Kaluzny & Rucinski (1995) diagram systematically “redder” in $(U - B)$ color. To overcome our saturation problems with the brightest B magnitudes, however, we cross-identified all of our bright-end B magnitude sample with the Kaluzny & Rucinski (1995) catalog, and use the latter source for all $B \leq 15.55$ mag objects across our field, providing to consistently correct the Kaluzny & Rucinski (1995) photometry to our magnitude scale according to Fig. 2. As a result, the CMD in the right panel of Fig. 5 matches our own photometry for stars fainter than $B = 15.55$ mag, and the (revised) Kaluzny & Rucinski (1995) photometry, for the 110 objects brighter than this magnitude limit. All over, our global NGC 6791 catalog consists of 7840 entries and its resulting CMD is consistently the same as in the Buzzoni et al. (2012) analysis. Overall, note from Fig. 5 that our photometry turns out to be over one magnitude deeper than Kaluzny & Rucinski (1995) reaching the WD region at the faint-end tail of magnitude distribution, about $B \sim 22.5$.

A comparison of our CMD with the YZVAR Padova isochrone set (Bertelli et al. 2008), as in the right panel of Fig. 5, helps us constrain the overall evolutionary properties of the cluster. For a chemical mix $(Z, Y) = (0.04, 0.30)$ the observed CMD confirms a consensus age between 6 and 8 Gyr (Anthony-Twarog et al. 2007; Buzzoni et al. 2012), providing to shift models to an apparent B distance modulus $(m - M)_B = 13.6$ mag, and assume a color excess $E(U - B) = 0.13$.

In the same Fig. 5, we encircled in both CMDs the 19 hot-star candidates proposed by Kaluzny & Rucinski (1995, see Tables 1 and 2, therein). The sub-group of WDs is easily recognized fainter than $B \sim 19.5$, while an obvious EHB candidates clump stands out around $B \sim 18$. Of these, stars B01 and B07 in the Kaluzny & Rucinski (1995) original list are controversial cases claimed to be field stars by Liebert et al. (1994) according to radial velocity measurements, but recently re-classified as likely members of the cluster by Platais et al. (2011) based on their new astrometric analysis. The case of star B10 is also a further controversial one as, according to Kaluzny & Rucinski (1995), this object is a blend of two stars with $\Delta V \sim 2$ mag and it is questioned as a likely field interloper by Platais et al. (2011). After careful inspection, object B10 can confidently be resolved in our frames, and we are inclined to assign cluster membership

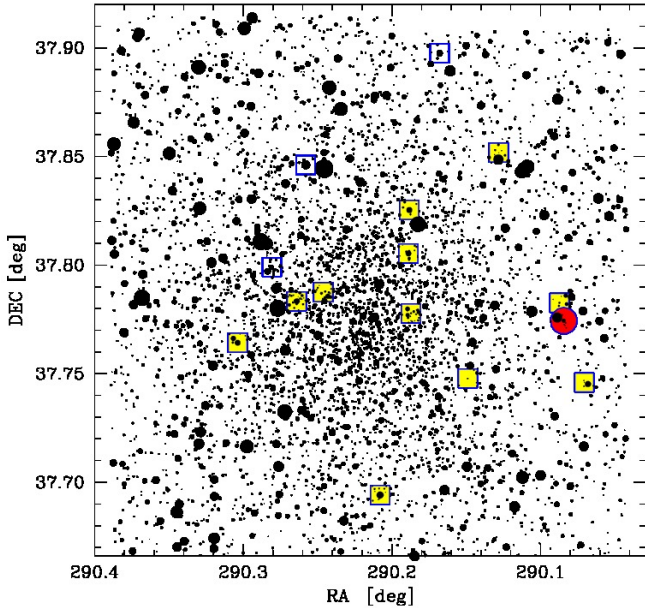


FIG. 6.— The new EHB candidate proposed in this study is located here on the cluster map of NGC 6791 (big red solid dot) together with the Kaluzny & Rucinski (1995) hot-star sample, as from Fig. 5 (square markers). The questioned member stars, B01 and B07 and B10, are singled out with open squares.

TABLE 4
EHB CANDIDATES IN THE FIELD OF NGC 6791

ID	R.A. (J2000.0)	DEC	B	(U-B)	KR95
NGC 6791					
377	19:20:40.33	37:53:50.9	16.98(0.02)	-0.43(0.03)	B01
411	19:20:49.92	37:41:39.0	17.25(0.02)	-1.12(0.03)	B02
554	19:20:45.19	37:49:31.5	17.61(0.02)	-0.96(0.04)	B03
585	19:21:12.91	37:45:51.3	17.69(0.02)	-0.96(0.04)	B04
606	19:21:03.36	37:46:59.8	17.73(0.02)	-0.93(0.04)	B05
644	19:20:45.34	37:48:19.5	17.80(0.02)	-1.03(0.04)	B06
1379	19:21:07.41	37:47:56.5	18.40(0.02)	-0.70(0.04)	B07
5939	19:20:35.74	37:44:52.3	21.07(0.03)	-1.15(0.05)	B08
156	19:21:01.92	37:50:46.2	16.20(0.01)	-0.78(0.02)	B10
1812	19:20:20.22	37:46:27.6	18.63(0.02)	-0.84(0.04)	...

Notes: KR95 = ID no. from Kaluzny & Rucinski (1995).

at least to the brightest component of the blend.

Following Buzzoni et al. (2012), one more star should be included to this EHB sample. This is target B08 in the Kaluzny & Rucinski (1995) notation, the most UV-enhanced object in our sample. In spite of its much fainter apparent B magnitude, in fact, this star is the hottest object in our catalog, which implies a much larger intrinsic luminosity, after bolometric correction, fully consistent with its location in the high-temperature extension of the cluster HB (see Fig. 3 in Buzzoni et al. 2012). Star B08 partly escaped its peculiar location in the original CMD of Kaluzny & Rucinski (1995) (see left panel of Fig. 5) due to a redder color, mainly in consequence of a ~ 1 brighter B magnitude, compared to our photometry. Such a notable difference urged a thorough check on our TNG frames to manually probe apparent U and B magnitudes. A supplementary check was also carried out for star B16, which we see ~ 0.8 fainter in B than Kaluzny & Rucinski (1995). After careful inspection, for both cases we can fully confirm our magnitude estimates of Table 4 and 5, thus attributing most of the

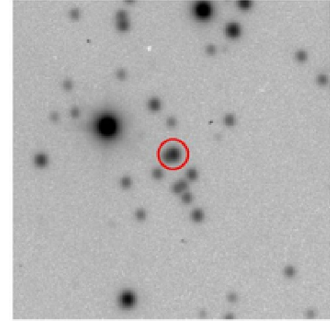


FIG. 7.— The B -band finding charts for the new EHB candidate in NGC 6791 proposed in this study. This is star ID #1812 in our catalog. Chart is $1' \times 1'$ across, centered at the coordinates of Table 4. North is up, East to the left.

TABLE 5
OTHER CROSS-REFERENCED FAINT HOT STARS IN THE FIELD OF NGC 6791, ACCORDING TO KALUZNY & RUCINSKI (1995)

ID	R.A. (J2000.0)	DEC	B	(U-B)	KR95
6684	19:20:30.78	37:51:06.2	21.63(0.03)	-0.54(0.05)	B11
6995	19:20:59.08	37:47:15.1	21.94(0.03)	-0.17(0.05)	B14
4801	19:20:20.90	37:46:57.4	20.34(0.03)	-0.92(0.05)	B15
4784	19:20:44.92	37:46:40.2	20.33(0.03)	-0.87(0.05)	B16
7068	19:20:16.92	37:44:46.2	22.02(0.04)	-0.92(0.06)	B18

Notes: KR95 = ID no. from Kaluzny & Rucinski (1995).

apparent discrepancy to the Kaluzny & Rucinski (1995) photometry.

Overall, according to our survey, we could only detect 14 out of the 19 hot-star candidates of Kaluzny & Rucinski (1995) since 5 of them (namely B09, B12, B13, B17 and B19) happen to fall outside our field of view. The cross-identification of the 9 Kaluzny & Rucinski (1995) EHB candidates in our sample is reported in Table 4, together with accurate J2000.0 coordinates, B magnitude and $(U - B)$ color according to our observations. For reader's better convenience, the remaining 5 stars in our field are summarized in Table 5. The position of all the 14 hot stars in common with Kaluzny & Rucinski (1995) is indicated in the cluster map of Fig. 6.

In addition to the 9 *bona fide* EHB stars in the Kaluzny & Rucinski (1995) list, a further new candidate, that escaped any previous detection— i.e. entry #1812 in the present catalog, aka star “c” in Fig. 3 of Buzzoni et al. (2012)— should be added to the EHB sample. Its dereddened $(U - B)$ color suggests for it a temperature of $T_{\text{eff}} \simeq 22,300$ K (Buzzoni et al. 2012). This star is reported in Table 4 and marked as a big red dot in our CMD of Fig. 5 (right panel) and in the cluster map of Fig. 6. A more detailed finding chart, for future observing reference, is also reported in Fig. 7. Although not confirmed spectroscopically, the projected distance from the cluster center makes this target compatible with its possible membership to the system. This statistical argument will be further detailed in Sec. 4, leading us to attach this star a $> 70\%$ membership probability.

Based on our revised star catalog, we also carefully reconsidered the nature of the striking clump of UV-strong stars, about $B \sim 15.5$, preliminarily appeared in the CMD of NGC 6791, as shown in Buson et al. (2006, see Fig. 2 therein). Although clearly detected on the deep U imaging frames, these objects stand out in our orig-

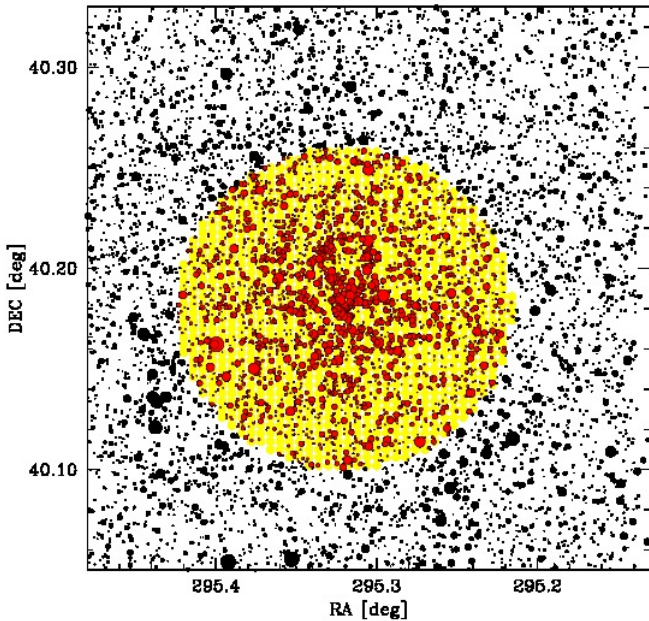


FIG. 8.— Overall map of the surveyed field across NGC 6819. The central spot locates the “inner” region of 5 arcmin radius surrounding the cluster center. Some very bright stars East to the cluster have been masked (see Fig. 1) preventing accurate photometry in the relatively close region.

inal photometric catalog for their large B photometric error, a feature that led us to suspect some intervening saturation effect in this band. For this reason an “*ad hoc*” individual recognition of this bright sample on the original TNG images has been carried out together with an independent cross-identification of each target in the Kaluzny & Rucinski (1995) B catalog. Our perception actually did turn out to be correct and, after recovering CCD saturation, we were unable to isolate in NGC 6791 any additional (clump of) UV-bright stars.³

Overall, across our field of view, the open cluster NGC 6791 seems therefore to host a total of ten EHB stars.

3.2. NGC 6819

This study presents the first-ever U CCD photometry for this cluster. Down to $B = 24.0$, our photometric catalog collects a total of 6504 objects. The system looks very concentrated spatially with a substantial fraction of its stellar population comprised within a radius of $\sim 5'$ from the center (see Fig. 8). According to the star number-density distribution, the latter can be located at $(\alpha; \delta)_{2000.0} \simeq (19^{\text{h}}41^{\text{m}}17^{\text{s}}; +40^{\circ}10'47'')$.

The CMD of the 2413 stars within the “inner” region (Fig. 9, upper panel) shows a well populated stellar main sequence (MS), that neatly shows up against the Galactic background. Also a red clump of HB stars, about 1 mag brighter than the Turn Off (TO) point, is clearly visible in the figure, about $(U - B) \sim 1.4$. One can also notice the TO region to display an evident “hooked” pattern pertinent to stars of $M \gtrsim 1.4 M_{\odot}$ growing a convective core inside. This is evocative of stellar populations of intermediate age. Actually, a tentative match of the “inner” CMD with the Padova isochrones (Bertelli et al.

³ Similarly, the saturation check also led us to reject two additional hot-star candidates of Buzzoni et al. (2012, see labelled objects “a” and “b” of Fig. 3 therein).

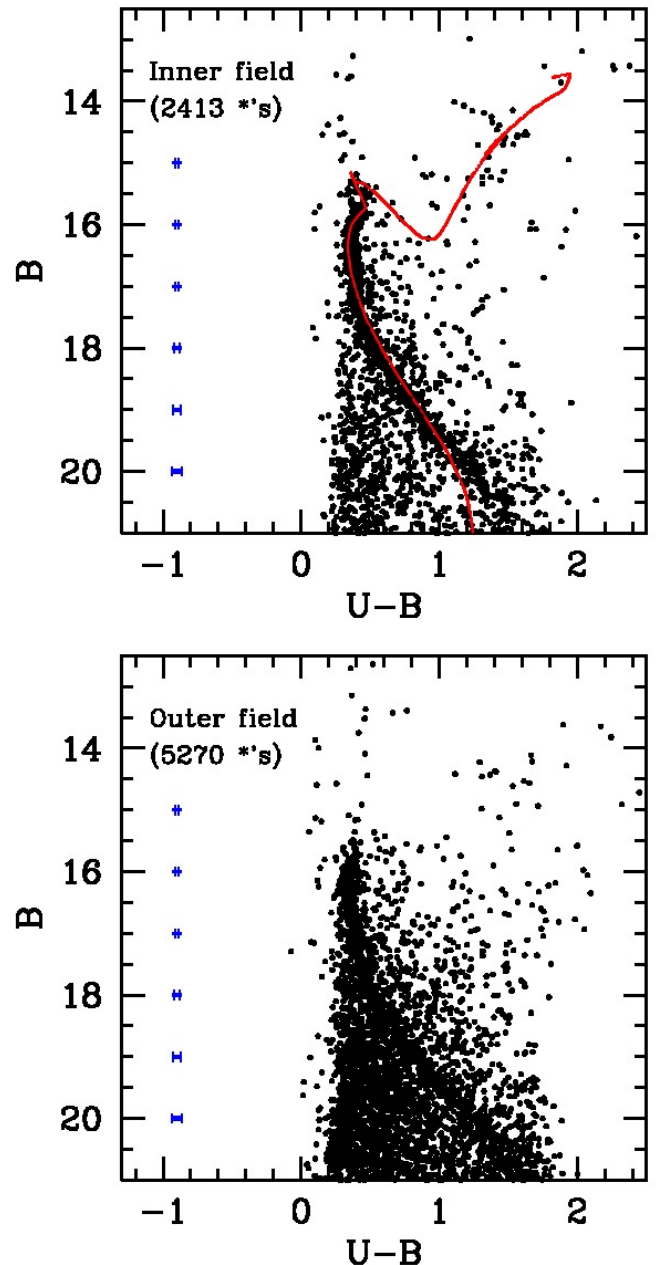


FIG. 9.— *Upper panel*: the B versus $(U - B)$ CMD of the “inner” region (within $5'$ from the cluster center) of NGC 6819. A total of 2413 stars brighter than $B = 24.0$ are displayed, as labelled. Note the “hooked” Turn Off pattern about $B \simeq 15.5$ and the red clump of HB stars, about 1 mag brighter, about $(U - B) \sim 1.4$. A tentative match with the 3 Gyr Padova isochrone (Bertelli et al. 2008) is displayed for $(Z, Y) = (0.04, 0.30)$. We imposed an apparent B distance modulus $(m - M)_B = 12.0$ mag and a color excess $E(U - B) = 0.15$. *Lower panel*: same plot but for stars in the “outer” region of the field, that is beyond $5'$ from cluster center (5270 objects in total, within the same magnitude limit). For both panels, typical error bars for our photometry at the different magnitude levels are displayed on the left.

2008) for $(Z, Y) = (0.04, 0.30)$ (see again the upper panel of Fig. 9) points to an age of ~ 3 Gyr, after reddening models for a color excess $E(U - B) = 0.15$ and assuming an apparent B distance modulus $(m - M)_B = 12.0$ mag for the cluster.

Interestingly enough, the MS stellar distribution seems to vanish toward lower luminosities with a clear defi-

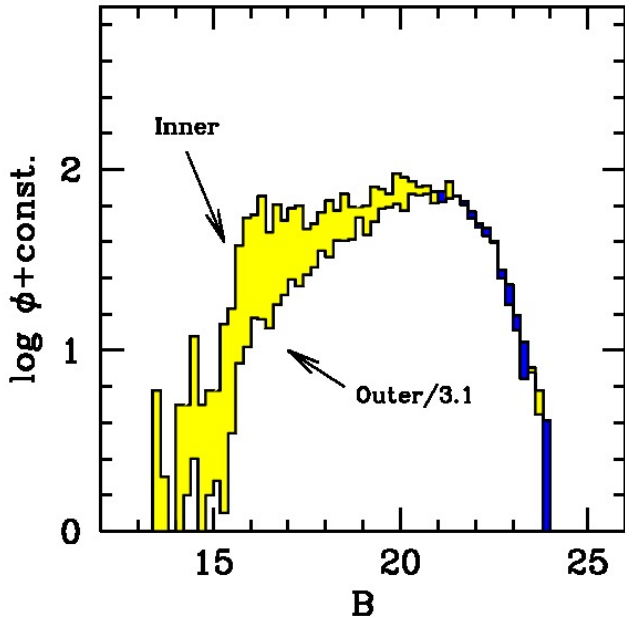


FIG. 10.— The apparent B -luminosity function of the “inner” and “outer” regions across the NGC 6819 field. To consistently compare the two regions, “outer” star counts have been reduced by a factor of ~ 3.1 to rescale to the same area as for the “inner” region. Note the inner residual excess of bright red giants and upper-MS stars and the lack of any central concentration for the low-MS stellar distribution fainter than $B \sim 20$.

ciency of stars fainter than $B \sim 20$. A comparison with the observed field star counts, at the same magnitude level, definitely rules out any possible bias due to incomplete sampling and points therefore to an inherently “flat” (i.e. giant-dominated, in the mass range $1.02 - 1.17M_{\odot}$) or truncated IMF for the cluster stellar population.

Although much more blurred and heavily perturbed by field star interlopers, all these features of the CMD can also be recognized in the corresponding plot of the 5270 stars across the “outer” region ($r > 5'$ in Fig. 8), as in the lower panel of Fig. 9. This clearly points to a much larger extension of the NGC 6819 system itself, as found indeed by Kalirai et al. (2001), who placed the cluster edge $\sim 9.5'$ away from the center.

Once rescaled to the same area across the sky, the apparent luminosity function of the “inner” and “outer” regions in NGC 6819 can consistently be compared, as in Fig. 10. Supposing the Galaxy background to be uniformly distributed across the field, then the residual excess of bright red giants and upper-MS stars in the innermost region effectively traces the cluster stellar population. In addition, the plot also confirms that cluster low-MS stars fainter than $B \sim 20$ are spread out across the field and do not show any central concentration. Our evidence fully supports the results of Kalirai et al. (2001), who pointed out the prevailing presence of low-mass stars ($M \lesssim 0.65M_{\odot}$) in the outer regions of the cluster.

3.3. NGC 7142

As for NGC 6819, also for this cluster we are presenting here the first U -band CCD photometry ever. A total of 3422 stars have been measured, brighter than $B = 24.0$. The cluster does not clearly stand against the field, and looks very contaminated. This reinforces the idea

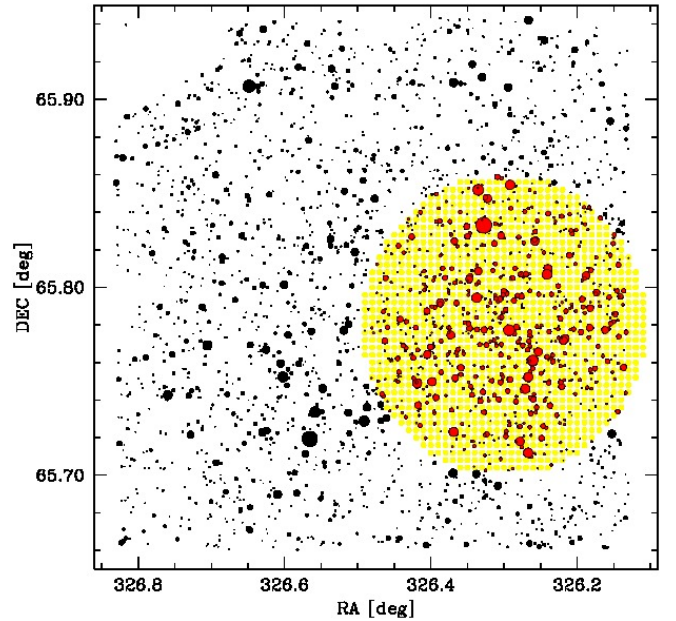


FIG. 11.— Overall map of the surveyed field across NGC 7142. The central spot locates the “inner” region of 5 arcmin radius surrounding the cluster center. A bright star North-East to the cluster has been masked (see Fig. 1) thus preventing accurate photometry in the relatively close region.

that NGC 7142 is a loose open cluster on the verge of dissolving into Galactic disk (van den Bergh & Heeringa 1970).

The stellar locus in the B vs. $(U - B)$ plane can be enhanced by restraining our display to the densest innermost region of the system. For this reason we collected stars into a circular region within a $5'$ radius around the cluster center, the latter assumed to coincide with the peak of the star number density, roughly located at $(\alpha; \delta)_{2000.0} \simeq (21^{\text{h}}45^{\text{m}}11^{\text{s}}; +65^{\circ}46'49'')$ (see Fig. 11). This “inner” sample consists of 1087 stars and evidently maximizes the fraction of cluster members. Its CMD (upper panel of Fig. 12) can be contrasted with the “outer” stellar distribution across the surrounding field, amounting to a total of 2335 stars (lower panel of the figure).

The cluster MS neatly appears in the upper panel of the figure, with the TO point located at $[B, (U - B)] \sim [16.5, 0.3]$. The MS smoothly connects with a coarse but extended RGB that tips about $[B, (U - B)] \sim [14.0, 2.3]$. As for NGC 6819, the diagnostic match with the Bertelli et al. (2008) Padova isochrones provides very similar results pointing however to an age of roughly 4 Gyr (see upper panel of Fig. 12). As for NGC 6819, no clear evidence for any possible hot stellar component to be related with the cluster population seems to emerge from the analysis of our CMD.

By further extending the comparison with NGC 6819, a notable feature one has also to remark from the CMDs of Fig. 12 is an inherent deficiency of faint low-MS stars below $B \sim 20$. This feature becomes even more evident as far as the cluster luminosity function is assessed, although on a merely statistical basis, in terms of star count excess vs. B apparent magnitude of the ‘inner’ versus ‘outer’ sample, as shown in Fig. 13. Such a vanishing MS, together with the overall loose morphology of the cluster, may consistently fit with a dynamical scenario modulated by the Galaxy interaction. Faint low-mass

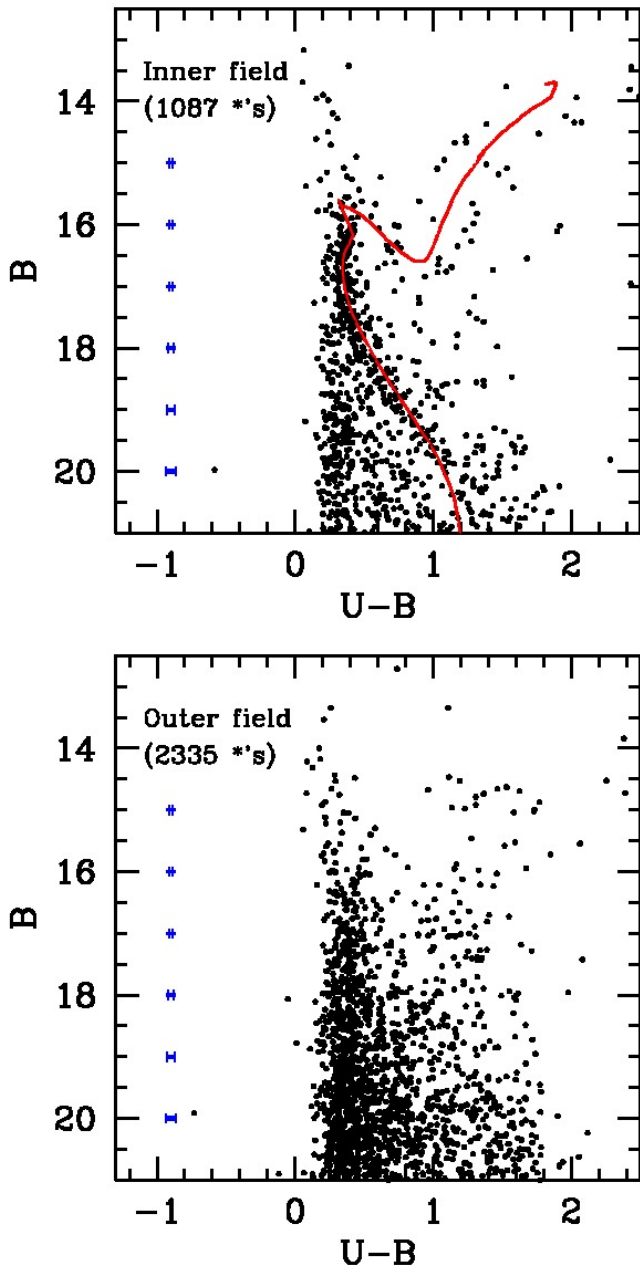


FIG. 12.— Same as for Fig. 9, but for cluster NGC 7142. In order to enhance cluster visibility, the upper panel collects photometry for 1087 stars brighter than $B = 24.0$ in an “inner” region within 5 arcmin from cluster fiducial center, as in the map of Fig. 11, while the field distribution in the “outer” region (2335 stars) is displayed in the lower panel. A match is attempted in the upper panel with a 4 Gyr Padova isochrone (Bertelli et al. 2008) for $(Z, Y) = (0.04, 0.30)$. An apparent B distance modulus $(m - M)_B = 12.0$ mag and a color excess $E(U - B) = 0.10$ is assumed to rescale models. For both panels, typical error bars for our photometry at the different magnitude levels are displayed on the left.

stars should, in fact, be the first and most affected by Galaxy tidal stripping over cluster lifetime (McLaughlin & Fall (2008)). On the other hand, likewise NGC 6819, an apparent lack of low-mass stars could also be the tricky by-product of a prevailing fraction of binary (multiple?) stellar systems within the cluster population. If this is the case, then the entire MS locus might be affected leading, among others, to a younger inferred age

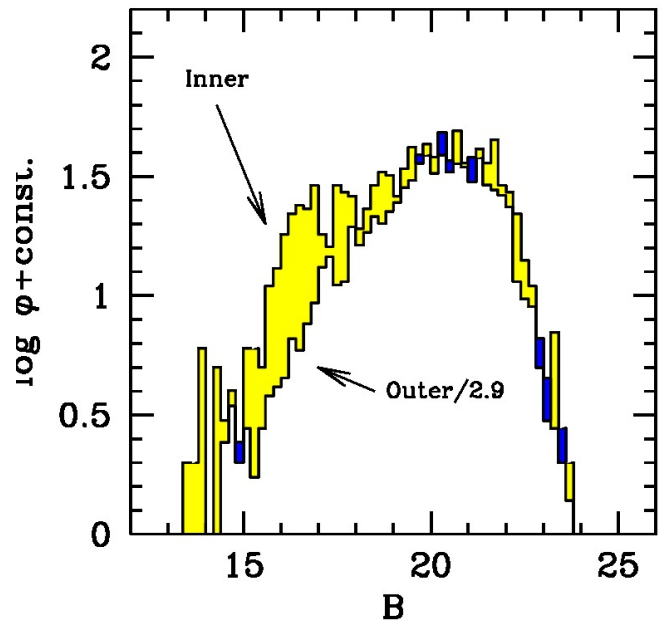


FIG. 13.— Same as for Fig. 10, but for cluster NGC 7142. Again, to consistently compare the “outer” and “inner” areas, star counts in the external region have been rescaled by a factor of ~ 2.9 , as labelled in the plot.

for the cluster, as probed by a brighter TO point.

4. CLUSTER MEMBERSHIP AND FIELD STAR CONTAMINATION

Thanks to the large covered field, and the quite low ($b \simeq 8-11^\circ$) Galactic latitude, a substantial fraction of disk stellar interlopers is expected to affect our open-cluster observations. To independently probe the Galaxy contamination along our pointing directions, and eventually assess, on a firmer statistical basis, cluster membership of the observed stars in each cluster, we therefore made a Monte Carlo experiment relying on the Girardi et al. (2005) Galactic model to compute synthetic CMDs of the relevant sky regions. To make our realizations statistically significant, we ran several trials with varying the random seed, and then we smeared the synthetic CMDs by adding photometric errors as from our observations, according to Fig. 4. Finally, reddening at infinity has been applied to the theoretical $(U - B)$ colors, following Schlegel et al. (1998).

The synthetic field realizations along the line of sight of NGC 6791, 6819 and 7142 are displayed in the three left panels of Fig. 14, as labelled on the plots. To ease a direct comparison with the corresponding CMDs of Fig. 9 and 12, where lower panels better probe the field in the off-center region of the clusters, we scaled our simulations to match a similar area coverage on the sky (namely ~ 0.06 square degrees). The contribution of the different Galaxy components is color coded in the plots of Fig. 14, with halo stars in red, thin disk stars in green and thick disk stars in blue. Consistently with the low Galactic latitude of our clusters, one can notice that thick-disk stars are by far the prevailing contributors throughout.⁴ For each cluster, in the the right panels of Fig. 14 we

⁴ According to Girardi et al. (2005) an exponential radial density profile is assumed for the thick-disk stellar component in the model, with a scale length of 2.8 kpc.

also compared the B -luminosity functions, as observed across the “outer” regions of the three fields (thick-line histograms overplotted in each panel), with the corresponding Monte Carlo output.⁵ As expected, cluster NGC 6791 and NGC 6819 are easily recognized to “spill over” the 5′ region in the CMDs of Fig. 5 and 9 and induce a star count excess in the field luminosity function. This is not the case for NGC 7142 which, on the contrary, seems to be fully contained within the inner 5′ spot of Fig. 11.

Cluster membership of stars within the “inner” regions of our frames can be statistically assessed by taking advantage of the Milky Way synthetic templates and relying on the Mighell et al. (1998) procedure. Restraining our test to stars brighter than $B \sim 20$ we have that, on average, about 78% of the objects in the “inner” region of NGC 6791 can confidently be cluster members. A similar figure is obtained for NGC 6819, leading to a membership fraction of 71% within the inner 5′ radius. Due to its vanishing profile, the case of NGC 7142 is much worse suggesting that the cluster actually consists of a mere 28% of the “inner” stars.

As far as the distinctive properties of the Galaxy field are concerned, at least three interesting differences seem to emerge from the comparison of our “outer” stellar samples and the Girardi et al. (2005) synthesis model of Fig. 14. More specifically:

i) Even considering the smearing effect of photometric errors, still a much broader extension toward “redder” colors has to be reported for our observations, with a larger fraction of faint ($B \gtrsim 18$) objects exceeding $(U - B) \gtrsim 1.5$, as shown in the CMDs of Figs. 5, 9, and 12. Distant galaxies in the background, like high-redshift ellipticals, may be an issue in this regard as they extend in apparent color well redder than Galactic M-type dwarfs. However, also differential reddening effects may give reason of this apparent discrepancy. A check in this sense has been carried out by relying on the relative shift of the MS locus in the cluster CMD across the field of view, as explained in von Braun & Mateo (2001). No sign of “patched” reddening is found across NGC 6819 and NGC 7142, although within a rough ($\Delta E(U - B) \sim \pm 0.1$ mag) internal uncertainty of our procedure due to poor statistics. Just a marginal (though cleaner) evidence of a reddening gradient appears, on the contrary, for NGC 6791, with hints for $E(U - B)$ to slightly increase by $\sim 0.05 \pm 0.04$ mag toward the East edge of the field.

ii) As far as the luminosity function is concerned (see the left panels of Fig. 14), the bright-end stellar distribution of the Girardi et al. (2005) model tends to predict all the way a more sizeable fraction of very bright ($B \lesssim 13$) (thick-disk) stars, not present in the same amount in our stellar samples.⁶

iii) Finally, and even more importantly, an enhanced population of WDs (of both thick- and thin-disk origin)

⁵ The same selection is adopted for NGC 6791, for which we probed the B luminosity function for stars across the map of Fig. 6 located 5′ or more away from the cluster center, the latter assumed to coincide with the peak of the star number density at $(\alpha; \delta)_{2000.0} \simeq (19^h 20^m 52^s; +37^\circ 46' 13'')$.

⁶ One has to notice, however, that we are somewhat biased against the selection of very bright stars in our photometric catalogues.

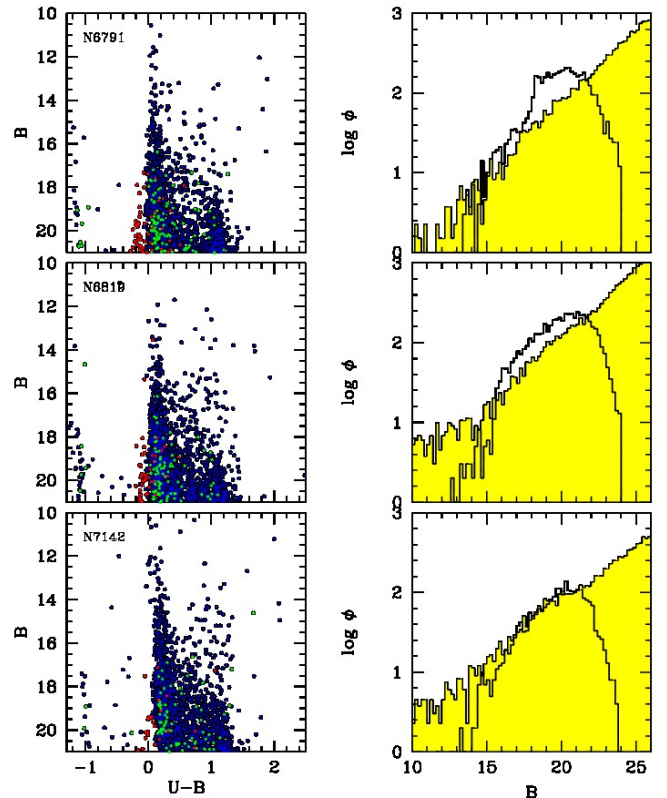


FIG. 14.— Field realizations along the line of sight of NGC 6791, 6819 and 7142 simulated by means of the Girardi et al. (2005) Galactic model. The synthesis output has been scaled throughout to an area of 0.06 square deg in order to consistently match the observed stellar sample of our “outer”-field regions (as in the maps of Fig. 8 and 11, for instance). The synthetic CMDs are displayed in the left panels, while the corresponding B -band luminosity function are computed in the right panels, and compared with our “outer” observations on a similar area of the clusters (thick-line histograms). Color code in the synthetic CMDs is red for halo stars, green for the thin disk, and blue for the thick disk. Note, all the way, the prevailing contribution of thick-disk stars to the coarse Galactic field.

is predicted in all the three fields with a clear sequence of faint ($B \gtrsim 18$) UV-strong objects “bluer” than $(U - B) \sim -1$. Puzzling enough, observations show no sign of such a sizeable field WD population, at least in the line of sight of NGC 6819 and 7142, while only a marginal evidence might perhaps tackle the nature of the few faintest UV stars in NGC 6791. Altogether, points *(ii)* and *(iii)* may be a hint for the Girardi et al. (2005) theoretical scheme to further tune up its assumed thick-disk morphology pointing to a shorter scale length, such as to reduce the overwhelming presence of relatively close (bright) stars and their progeny of WDs in the solar neighborhood.

5. SUMMARY AND DISCUSSION

We reported on a multiple, UV-oriented survey in the fields of the open clusters NGC 6791, NGC 6819 and NGC 7142, which—owing to their super-solar metal content and estimated old age—represent both very near and ideal stellar aggregates to match the distinctive properties of the evolved stellar populations, possibly ruling the UV-upturn phenomenon in elliptical galaxies and bulges of spirals. To this goal we made use of TNG U, B imagery.

For each cluster, the resulting B vs. $(U - B)$ CMD fairly well matches the fiducial evolutionary parameters as pro-

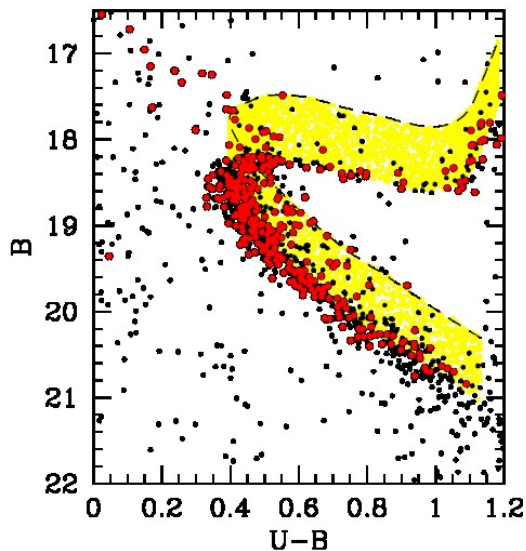


FIG. 15.— A zoomed-in CMD of NGC 6791 around the MS turn-off region. Only stars in our catalog within a $2.5'$ radius from cluster center have been considered, in order to minimize the field-star contamination. According to Cudworth (2008, private communication, as cited by Twarog et al. 2011) stars with membership probability $P_m \geq 80\%$ have been marked by big red dots. Dashed curve is the MS fiducial locus shifted toward 0.75 mag brighter luminosities such as to edge any MS+MS star pair in case of unresolved binary systems. See text for details.

posed in the recent literature, a fact that further corroborates the quality of our dataset. In particular, taking the Padova suite of isochrones as a reference (Bertelli et al. 2008) for TO fitting, and owing to a super-solar metallicity for all the three clusters, we confirm for the NGC 6791 stellar population an age of 7 ± 1 Gyr, while slightly younger figures, i.e. 3 and 4 Gyr, may be more appropriate for NGC 6819 and 7142, respectively.

As already pointed out by Landsman et al. (1998), a bimodal HB morphology is clearly confirmed for NGC 6791, where the sizeable population of blue HB (BHB) stars accompanies the standard red clump (RHB) in a relative number partition of $[BHB : RHB] \sim [1 : 4]$. By relying on the observed HB distribution and the overall CMD morphology, a spectral synthesis of the cluster stellar population led Buzzoni et al. (2012) to emphasize the *unique role* of this NGC 6791 as a “morceau” of the metal-rich, evolved stellar populations characterizing the upturn-strong giant ellipticals. This conclusion finds out further support also by the direct experiments of Dorman et al. (1995) and Buzzoni & González-Lópezlira (2008), where the ultraviolet spectra of the strongest UV-upturn galaxies, together with other integrated spectral features, like the $H\beta$ strength, were actually reproduced in old metal-rich stellar environments with a relative fraction of 20-25% of BHB stars superposed to a canonical red HB evolution. As a further piece of evidence, stemming from the analysis of the NGC 6791 CMD, one may also recall the recent works of Bedin et al. (2008) and Twarog et al. (2011), where a similar figure (namely $\sim 30\% \pm 10\%$) is independently found for the fraction of binary stars in

this cluster. Once matching the membership probability, according to Cudworth proper-motion selection (as cited by Twarog et al. 2011) we also confirm this special feature of the NGC 6791 stellar population, as shown in Fig. 15. In order to minimize the field-star contamination, we restrained the stellar sample in the figure only to stars in our catalog within a $2.5'$ radius from cluster center. A “redward-blurred” distribution is clearly evident for the MS, with brighter and redder outliers all nicely comprised within an upper envelope 0.75 mag brighter than the fiducial MS locus, as expected indeed for these stars to be MS+MS star pairs. Such a sizeable presence of binary systems has actually been meant by Bedin et al. (2008) to originate the WD peculiar distribution as observed for this cluster. If this is the real case, then the apparent “excess” of EHB stars may actually be regarded as the key connection between MS and WD evolution.

Although clearly lacking any relevant hot stellar component, clusters NGC 6819 and 7142 might add further arguments on the same line. For both systems a vanishing and less concentrated low-MS stellar distribution (see Fig. 10 and 13) could be one possible consequence of an extended presence of binary (multiple?) stellar systems (the lack of faintest stars being due, in this case, to their “merging” into brightest integrated objects). Alternatively, one may call for a disruptive role of Galaxy tides on the dynamical evolution of these open clusters, with their low-mass stars to be the most easily stripped objects in consequence of Galaxy interaction.

The observation of the surrounding regions along the line of sight of each cluster allows us to usefully probe the Milky Way stellar field at low Galactic latitudes. Our data have been tackled by the theoretical Galaxy model of Girardi et al. (2005), that includes in some detail the photometric contribution of all the relevant stellar substructures, namely the spheroid system and the two thin- and thick-disk components. A match of the observed CMDs and B luminosity functions across our fields with the theoretical predictions of the model led us to conclude that a more centrally concentrated thick disk (with a scale length shorter than 2.8 kpc, as assumed by Girardi et al. (2005) might better reconcile the lower observed fraction of bright field stars and their WD progeny.

We would like to thank the anonymous referee for a careful reading of the draft and for a number of timely suggestions and recommendations, that greatly helped us refining our results. AB acknowledges the INAOE of Puebla for its warm hospitality, and the European Southern Observatory for awarding a visitorship to ESO premises in Santiago de Chile, where part of this work has been done. This project received partial financial support from the Italian Space Agency ASI, under grant ASI-INAF I/009/10/0 and from the Mexican SEP-CONACyT, under grant CB-2011-01-169554.

Facilities: TNG.

REFERENCES

- Anthony-Twarog B.J., Twarog B.A., & Mayer L. 2007, AJ, 133, 1585
 Auner, G. 1974, A&AS, 13, 143
 Bedin L. R., Salaris M., Piotto G., Cassisi S., Milone A. P., Anderson J., & King I. R., 2008, ApJ, 679, L29
 Bertelli G., Girardi L., Marigo P., Nasi E., 2008, A&A, 484, 815

- Bragaglia, A., Carretta, E., Gratton, R., Tosi, M., et al. 2001, *ApJ*, 121, 327
- Bragaglia, A., Tosi, M., 2006, *AJ*, 131, 1544
- Brown D., Yi S., Han Z., & Yoon S.-J., 2006, *Baltic Astronomy*, 15, 13
- Buson, L. M., Bertone, E., Buzzoni, A., & Carraro, G. 2006, *Baltic Astronomy*, 15, 49
- Buzzoni, A., Bertone, E., Carraro, G., & Buson, L.M., 2012, *ApJ*, 749, 35
- Buzzoni, A., & González-Lópezlira, R. A. 2008, *ApJ*, 686, 1007
- Carney B.W., Lee J-W., & Dodson B. 2005, *AJ*, 129, 656
- Carraro G., & Chiosi C. 1994, *A&A*, 287, 761
- Carraro G., Geisler, D., Villanova, S., Frinchaboy, P.M., & Majewski, S.R., 2007, *A&A*, 476, 217
- Carraro G., Girardi L., & Chiosi C. 1999, *MNRAS*, 309, 430
- Carraro G., Villanova S., Demarque P., McSwain M.V., Piotto G., & Bedin L.R. 2006, *ApJ*, 643, 1151
- Crinklaw, G., & Talbert, F.D. 1991, *PASP*, 103, 536
- Dorman, B., O'Connell, R.W., & Rood, R.T 1995, *ApJ*, 442, 105
- Girardi, L., Groenewegen, M. A. T., Hatziminaoglou, E., & da Costa, L. 2005, *A&A*, 436, 895
- Gratton R., Bragaglia A., Carretta E., & Tosi M., 2006, *ApJ* 642, 462
- Jacobson H.R., Friel E.D., & Pilachowski C.A. 2007, *AJ*, 134, 1216
- Jacobson H.R., Friel E.D., & Pilachowski C.A. 2008, *AJ*, 135, 2341
- Janes, K.A., & Hoq, S., 2011, *AJ*, 141, 92
- Kalirai J.S., Richer H.B., Fahlman G.G., Cuillandre J.-Ch., et al., 2001, *AJ*, 122, 266
- Kaluzny, J., & Rucinski S.M. 1995, *A&AS*, 114, 1
- Kaluzny, J., & Udalski, A. 1992, *AcA*, 42, 29
- Kinman, T.D. 1965, *ApJ*, 142, 655
- Landolt, A.U. 1992, *AJ*, 104, 340
- Landsman, W., Bohlin, R.C., Neff, S.G. et al. 1998, *AJ*, 116, 789
- Liebert, J., Saffer, R.A., & Green, E.M. 1994, *ApJ*, 107, 1408
- Lindoff, U. 1972, *A&AS*, 7, 497
- McLaughlin, D. E., & Fall, S.M. 2008, *ApJ*, 679, 1272
- Mighell, K. J., Sarajedini, A., & French, R. S. 1998, *AJ*, 116, 2395
- Montgomery, K. A., Janes, K. A., & Phelps, R. L. 1994, *AJ*, 108, 585
- Origlia L., Valenti E., Rich R.M., & Ferraro F.R. 2006, *ApJ*, 646, 499
- Origlia L., Rood R. T., Fabbri S., Ferraro F. R., Fusi Pecci F., & Rich R. M., 2007, *ApJ*, 667, L85
- Platais, I., Cudworth, K. M., Kozhurina-Platais, V., McLaughlin, D. E., Meibom, S., & Veillet, C. 2011, *ApJL*, 733, L1
- Rosvick, J.M., & Vandenberg, D.A., 1998, *AJ*, 115, 1516
- Schlegel, D.J., Finkbeiner, D.P., & Davis, M. 1998, *ApJ*, 500, 525
- Stetson, P.B., 1987, *PASP*, 99, 191
- Twarog, B. A., Ashman, K. M., & Anthony-Twarog, B. J. 1997, *AJ*, 114, 2556
- Twarog B. A., Carraro G., & Anthony-Twarog B. J., 2011, *ApJ*, 727, L7
- van den Bergh, S., Heeringa, R., 1970, *A&A*, 9, 209
- van den Bergh, S. 1962, *J.R.A.S. of Canada*, 56, 41
- van Loon J. T., 2006, *ASPC*, 353, 211
- von Braun, K., & Mateo, M. 2001, *AJ*, 121, 1522
- Warren S.R., & Cole A.A. 2009, *MNRAS*, 393, 272
- Yong, H., Demarque, P., & Yi, S. 2000, *ApJ*, 539, 928